

RAMAN SPECTROSCOPY AND MORPHOLOGY CHARACTERIZATIONS OF SWCNTs SYNTHESIZED BY KrF EXCIMER LASER ABLATION UNDER NEON GAS ATMOSPHERE

J. AL-ZANGANAWEE^{a,b}, T. MUBARAK^b, A. KATONA^a, C. MOISE^a, D. BALAN^a, D. DOROBANTU^a, D. BOJIN^a, M. ENACHESCU^{a,c,*}

^a*Center for Surface Science and Nanotechnology (CSSNT),*

Politehnica University of Bucharest, 060042, Romania

^b*Department of Physics, College of Science, University of Diyala, Diyala, Iraq*

^c*Academy of Romanian Scientists, Bucharest, Romania*

In this article, single wall carbon nanotubes (SWCNTs) were obtained by the KrF excimer laser ablation method in Neon gas atmosphere with 70 L/h flow rate at 500 Torr and temperature of 1100 °C. The target was prepared from a mixture of C/Ni/Co = 98.8/0.6/0.6 (atomic percentage). The ablation material was characterized by micro Raman spectroscopy, high resolution scanning transmission electron microscopy (HR-STEM), field emission scanning electron microscopy (FE-SEM) and thermogravimetric analysis (TGA). The ablated product contains SWCNTs, low amount of amorphous carbon and metallic catalyst nanoparticles. We found that the SWCNTs obtained are a mixture of semiconducting and metallic types. The SWCNTs in the raw material are organized in bundles and individual tubes with high length having the diameter in the range of 2.5- 42 nm for bundles and 1.0-1.7 nm for the individual tubes.

(Received March 2, 2016; Accepted May 13, 2016)

Keywords: Single wall carbon nanotube, Excimer laser ablation, Neon gas, Raman spectroscopy, HR-STEM, FE-SEM, EDX, and TGA

1. Introduction

Since their discovery in 1993 [1, 2], the single wall carbon nanotubes (SWCNTs), presented a great interest for the academic and industry world. Significant progresses have been made in the field of nanoscale science and technology, due to their unique chemical and physical properties, such as optical [3], mechanical and electrical [4]. Among the most important applications of SWCNTs we highlight the fabrication of field emission displays [5], atomic force microscope (AFM) tips [6], biosensors [7], hydrogen gas storage [8], and organic solar cells [9]. Over the years, different methods have been used for the fabrication of SWCNTs such as arc discharge [10], chemical vapor deposition (CVD) [11] and laser ablation [12]. Several types of carbon nanostructures can be obtained using laser ablation methods such as fullerene [13], nano-onions [14], and SWCNTs [15]. For the synthesis of high quality and yield of SWCNTs, the laser ablation proved to be an efficient method [16]. For the optimization of this method, the influence of various ablation parameters as temperature, target composition, laser beam wavelength, energy and repetition rate, pressure and flow rate of the carrier gas, and carrier gas type etc., have been studied [16,17]. There are several studies focused on the production of SWCNTs by excimer laser ablation using different carrier gas types as argon [18], nitrogen [19], and krypton [20].

In this study we describe the synthesis of fine-quality SWCNTs by KrF excimer laser ablation (248 nm) under Neon gas atmosphere. The ablation product was characterized by Raman micro-spectroscopy, FE-SEM, HR-STEM and TGA techniques.

* Corresponding author: marius.enachescu@upb.ro

2. Experimental work

The ablation experiment was carried out using a KrF excimer laser produced with a Coherent Compex Pro 205 equipment. The laser wavelength was 248 nm and the pulse period of 20 ns. The schematic custom-design of the installation used for producing SWCNTs is presented in the Figure 1 [18-20].

The experimental parameters were 550 mJ of laser energy, 30 Hz of laser repetition rate, 1h ablation time, 1100 °C furnace temperature, 500 Torr gas pressure, neon as carrier gas with 70 L/h flow rate. The target composition was C/Ni/Co = 98.8/0.6/0.6 (atomic percentage) prepared by an original recipe developed by Enachescu's group [18].

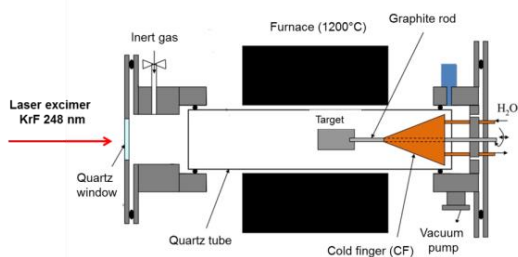


Fig.1. Experimental chamber design [18].

The experiment starts by passing the laser beam through an UV transparent quartz window from the left side of the chamber into the quartz tube where the temperature is 1100°C, hitting the rotating target. As a result, the target material starts to be ablated leading to the new product, such as SWCNTs. The ablated material from the target is transported by the Neon gas of 99.999% purity to a water cooled metallic body called cold finger (CF) where it is deposited as a black soot. The quartz tube of the reaction chamber is 1260 mm long, with the internal diameter of 50 mm. The flow rate of the carrier gas was 70 L/h. The cold finger was made of cooper.

After ablation, the raw product soot was collected from the copper cold finger. The morphology, structure, purity and diameter distributions of single wall carbon nanotubes in the raw product was investigated using micro-Raman spectroscopy, field emission electron microscope (FE-SEM), high resolution scanning transmission electron microscope (HR-STEM), and thermogravimetric analysis (TGA).

3. Result and discussion

3.1. Raman spectroscopy analysis

The Raman spectra of the ablation product were recorded using three different wavelengths of the laser: 633 nm, 532 nm, and 514 nm. We identified in the Raman spectra three bands as shown in the figure 2 corresponding to SWCNTs fingerprint: radial breathing mode (RBM) band, D band and G band [21]. From the RBM band we calculated the diameters distribution and conducting type of SWCNTs. From D band we estimated the purity and quality of SWCNTs, while from the G band we determined the conducting character of SWCNTs contained in the ablation product. In the followings, we present in detail our findings.

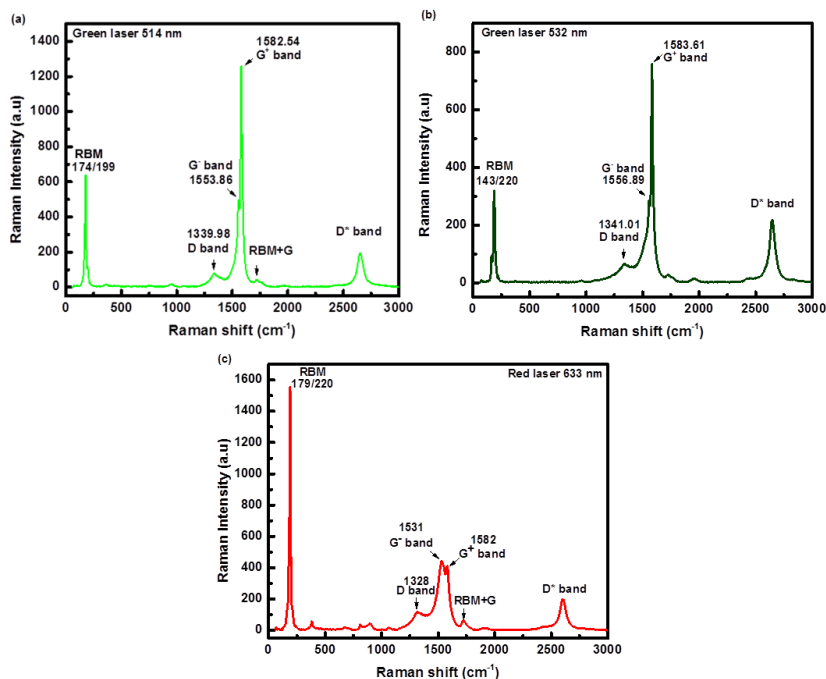


Fig. 2. Micro-Raman spectra of the raw ablation product. Excitation laser wavelengths of 514 (a), 532 (b), and 633 nm (c).

3.1.1. RBM band analysis

The corresponding RBM spectra to the three-excitation laser wavelengths are shown in figure 3. All curves were fitted with Lorentzian fitting.

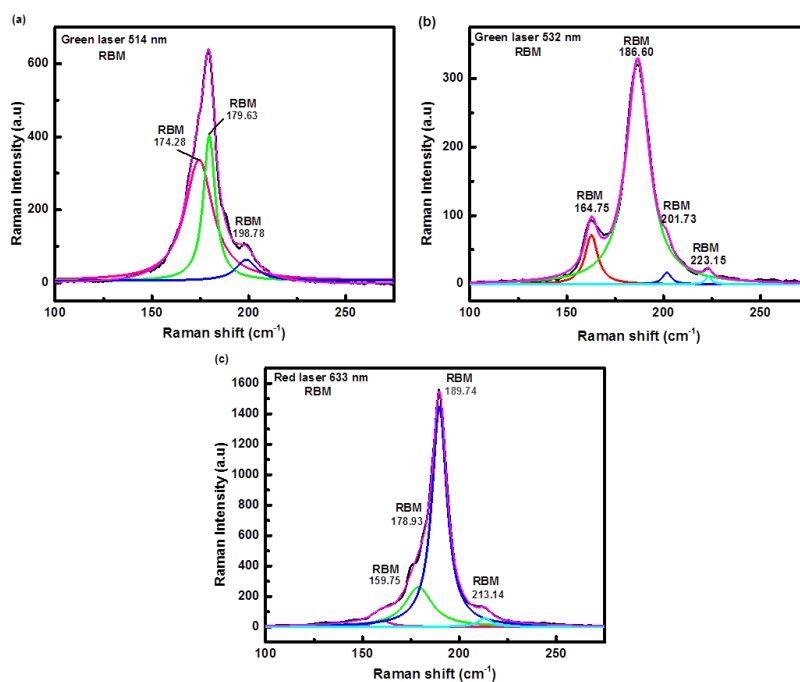


Fig. 3. Radial breathing mode (RBM) of the Raman spectra of the SWCNTs for three excitation laser wavelengths of 514 (a), 532 (b), and 633 nm (c). All curves were fitted with Lorentzian fitting.

The relationship between vibrational frequency in the radial direction of the tube and the diameter of the nanotube can be described by the equation 1 [22]:

$$d = c_1 / (\omega - c_2) \quad (1)$$

Where ω , c_1 , c_2 , and d , are the vibration frequency in the radial direction (cm^{-1}), constant (215 cm^{-1}), constant (18 cm^{-1}), diameter of the nanotubes [nm], respectively. We used equation 1 to calculate the diameter of the SWCNTs, the calculated data are enclosed in Table 1.

Table 1. RBM peaks position and calculated values of SWCNTs diameter and conducting character of the synthesized SWCNTs for three excitation laser wavelengths: 514, 532, and 633 nm.

Type of Laser	Position of peak (cm^{-1})	SWCNTs diameter (nm)	Type of SWCNTs
Green 514 nm (2.41 eV)	174.61	1.378	Semiconductor
	179.67	1.330	Semiconductor
	199.03	1.188	Metallic
Green 532 nm (2.33 eV)	162.722	1.487	Semiconductor
	186.607	1.356	Semiconductor
	201.731	1.170	Metallic
Red 633 nm (1.96 eV)	223.152	1.048	Metallic
	159.755	1.516	-----
	178.930	1.336	Metallic
	189.749	1.252	Metallic
	213.139	1.102	-----

The diameters distribution and its histogram for the SWCNTs are plotted in Figure 4 (a, b).

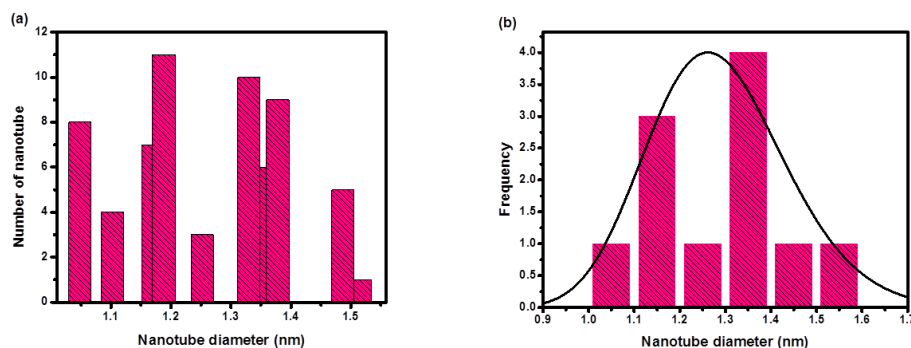


Fig. 4. (a) Diameters distribution of SWCNTs, and (b) Histogram of diameter distributions of the SWCNTs based on the analysis of micro-Raman spectra.

We found that the diameters distribution of the SWCNTs were in the range of 1.0 to 1.52 nm and centered on ~ 1.35 nm.

The semiconducting and metallic properties of the SWCNTs can be determined by using Kataura plot [23]. Kataura plot shows that the carbon nanotubes can be either semiconducting or metallic depending on its diameter [23].

The previously found SWCNTs diameters were overlapped in the Kataura plot to find the corresponding conducting character of the SWCNTs as shown in Figure 5.

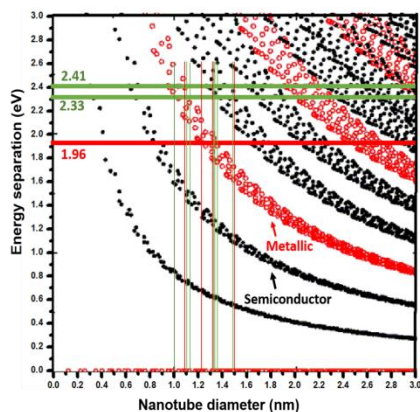


Fig. 5. The Kataura plot [21]. Black points are semiconductor nanotubes and red points are metallic nanotubes. three horizontal lines (One red laser with energy 1.96 eV (red line) and two green lasers with energies 2.33 eV and 2.41 eV (green line) were used as a excitation lasers in Raman measurements of SWCNTs. Vertical red and green lines indicate the diameters of SWCNTs.

According to Kataura plot we found a mixture of semiconducting and metallic SWCNTs as shown in Table 1.

3.1.2 D and G bands analysis

The corresponding D and G bands spectra to the three excitation laser wavelengths are shown in Figure 6. Lorentzian fitting was used for all the curves.

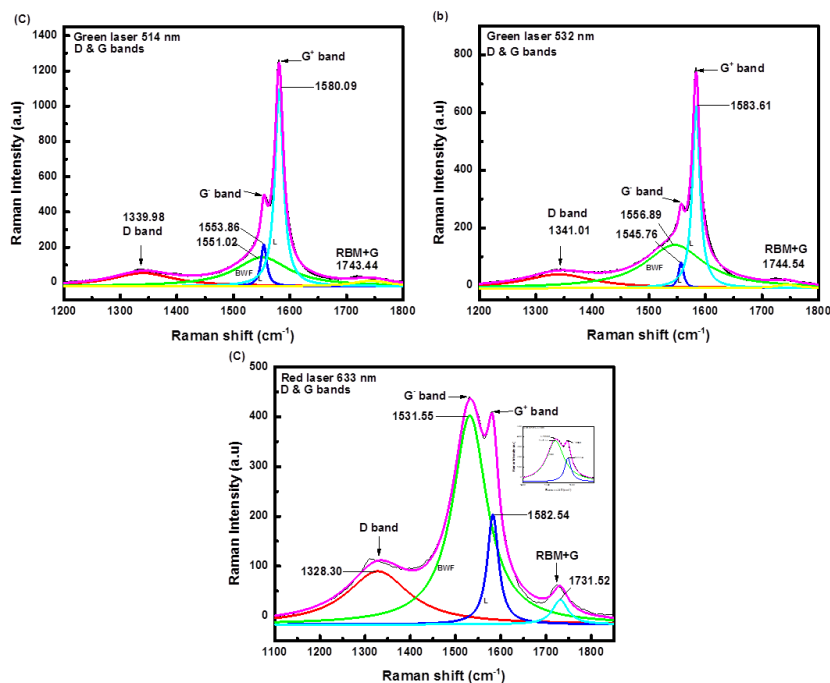


Fig. 6. D and G bands Raman spectra of the SWCNTs for three excitation laser wavelengths: 514 nm(a), 532 nm(b) and 633 nm(c). All curves were fitted with Lorentzian fitting.

From Figure 6 (a), the D band is fitted with one peak at 1339.98 cm^{-1} , and the G band of the synthesized SWCNTs is fitted with three line shape peaks, one broad metallic Breit-Wigner-Fano (BWF) line shape peak at 1551 cm^{-1} , and two narrow semiconducting Lorentzian line shape

peaks at 1554 and 1581 cm^{-1} [21]. As shown in Figure 6(b), the D band is fitted with one peak at 1341 cm^{-1} , and G band is fitted with one broad metallic Breit-Wigner-Fano (BWF) line shape peak at 1546 cm^{-1} and two Lorentzian lines shape peaks at 1557 and 1584 cm^{-1} . In the Figure 6(c), the Lorentzian fitting of D and G bands of the SWCNTs showed one broad metallic BWF line shape peak and one narrow semiconducting Lorentzian line shape at 1532 and 1584 cm^{-1} , respectively.

The I_D/I_G intensity ratio of the peaks is a measure of the SWCNTs quality, which shows the defects in the nanotube structure and the impurities attached to it [24].

The Lorentzian fitting positions of D, G⁻ and G⁺ bands, respectively the I_D/I_G intensity ratio are shown in Table 2.

Table 2. Lorentzian fitting positions of D, G⁻ and G⁺ bands, respectively the I_D/I_G intensity ratio of Raman spectra for the synthesized SWCNTs recorded with three excitation laser wavelengths: 514, 532, and 633 nm.

Type of Laser	Position of D band (cm^{-1})	Position of G band (cm^{-1})		I_D / I_G Intensity ratio
		G ⁻	G ⁺	
Green 514 nm (2.41eV)	1339.983	1551.025 1553.859	1580.991	0.067
Green 532 nm (2.33eV)	1341.013	1545.769 1556.889	1583.612	0.076
Red 633 nm (1.96 eV)	1328.297	1531.552	1582.645	0.250

The I_D/I_G intensity ratios present low values indicating the presence of good quality SWCNTs with low defects and attached impurities.

The results from deconvoluted G bands showed the obtained SWCNTs are a mixture of metallic and semiconducting types.

3.2. Field emission scanning electron microscope (FE-SEM) and high resolution scanning electron microscope (HR-STEM) analysis.

The ablation product was characterized using a Hitachi SU 8230 Ultra-high Resolution field emission scanning electron microscope (FE-SEM) and a Hitachi HD 2700 high resolution scanning electron microscope (HR-STEM).

3.2.1 FE-SEM analysis

FE-SEM images of raw ablation material are shown in the Figure 7. We found SWCNTs in the raw material which are organized into high density bundles with the length up to ~8 μm , having different diameters. In the close vicinity of the SWCNTs bundles we found amorphous carbon and catalysts metal nanoparticles. Using the FE-SEM images we measured the diameters of more than 100 bundles of SWCNTs. The plots of diameter distributions and their histogram have been done and shown in the Figure 8(a) and (b), respectively. The histogram diameter distributions of the SWCNTs bundles were in the range of 2.5–42 nm, and the center in ~7.5 nm.

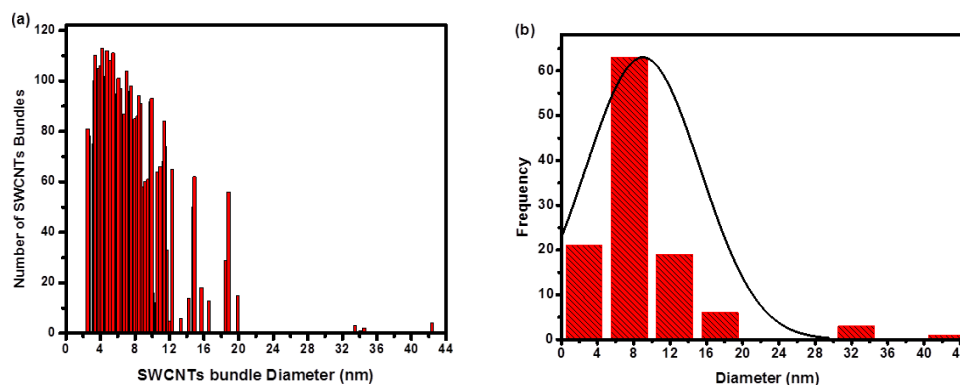


Fig. 8. (a) Diameters distribution of SWCNTs bundles, and (b) Histogram of the diameters distribution of SWCNTs bundles based on the FE-SEM observations.

3.2.2 HR-STEM analysis

High-resolution scanning transmission electron microscope (HR-STEM) images of the synthesized SWCNTs are shown in the Figure 9. We identified individual SWCNTs and bundles of SWCNTs, respectively the presence of amorphous carbon and catalysts metal nanoparticles (Co and Ni).

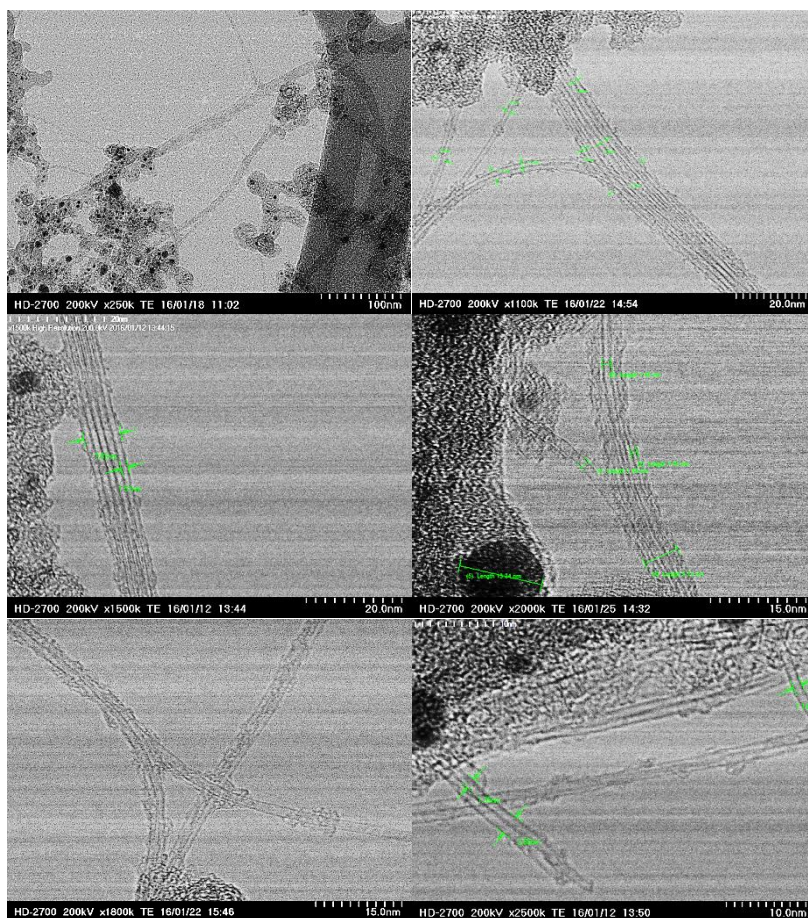


Fig. 9. High-resolution scanning transmission electron microscope (HR-STEM) images of the synthesized SWCNTs sample recorded at 200 kV.

We measured the diameters of 80 SWCNTs using HR-STEM images. The diameters distribution and its histogram are plotted in the Figure 10(a) and (b), respectively. The histogram of diameters distribution was in the range of 1.0 - 1.7 nm, and the center between 1.25 nm and 1.35 nm. This result is close to the result obtained from Raman measurements.

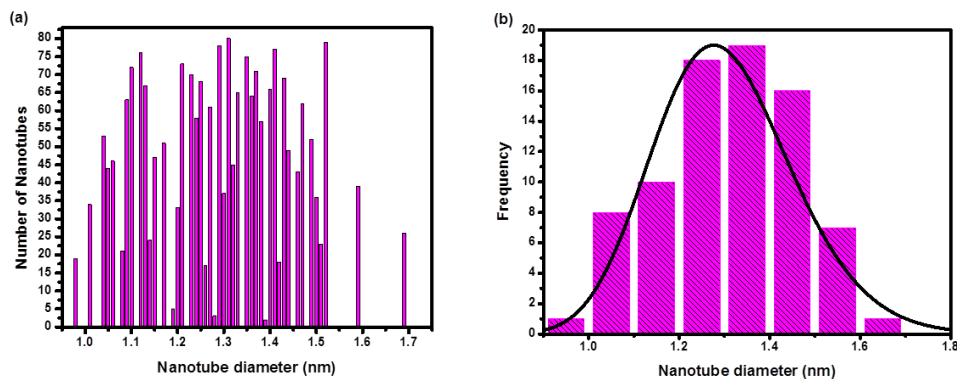


Fig. 10. (a) Diameters distribution of SWCNTs, and (b) Histograms of diameters distribution of the SWCNTs

Also, we measured the diameters of 80 SWCNTs bundles. Figure 11(a) and (b) show the diameters distribution and its histogram of these SWCNTs bundles. The histogram diameters distribution of the SWCNTs bundles was in the range of 2.65 – 11.4 nm, centered between 3.0 nm to 5.0 nm.

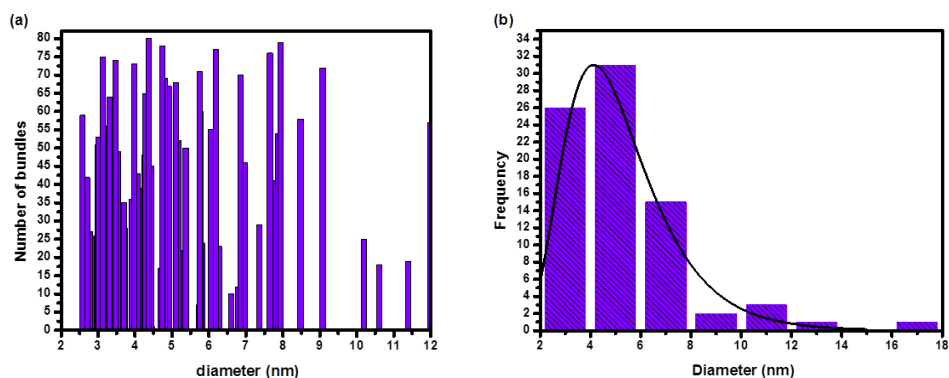


Fig. 11. (a) Diameters distribution of SWCNTs bundles, and (b) Histograms of diameters distribution of the SWCNTs bundles

The HR-STEM images show the presence of metal catalyst nanoparticles as Ni and Co, indicated by energy dispersive x-ray analysis (EDX), as shown in Figure 12.

Further, we measured the diameters of more than 100 catalyst nanoparticles. The diameters distribution and its histogram are shown in the Figure 13(a) and (b), respectively. The histogram of diameters distribution of catalyst nanoparticles was in the range of 1.6 to 19.75 nm, and centered on ~3.0 nm

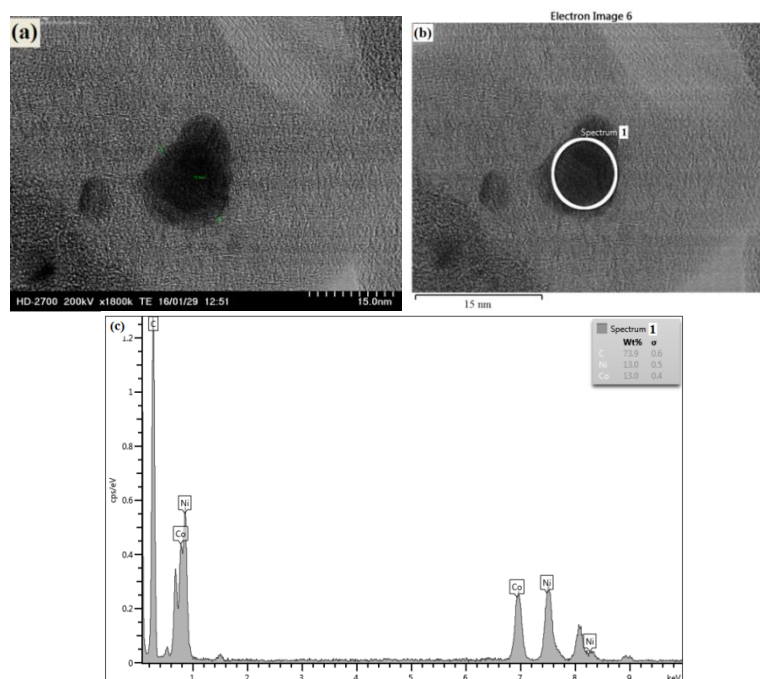


Fig.12. (a) HR-STEM image and (b) electron image of black nanoparticle in raw ablation material. (c) chart of energy-dispersive X-ray (EDX) analysis of the nanoparticle.

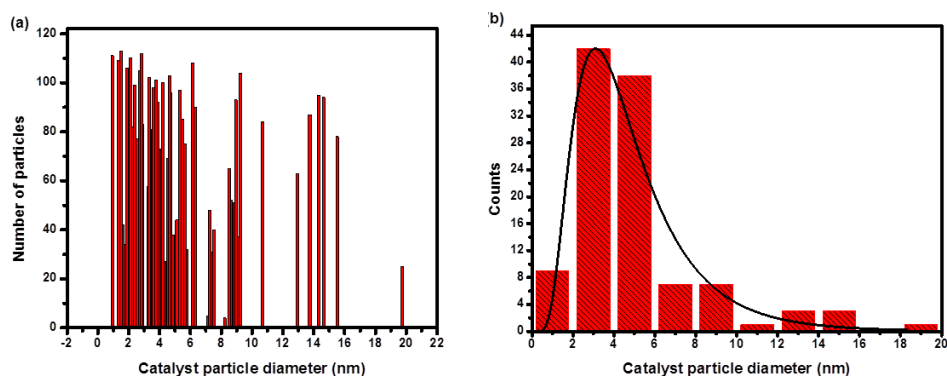


Fig. 13. (a) Diameters distribution of catalyst nanoparticles, and (b) Histogram of diameters distribution of catalyst nanoparticles based on the STEM observations.

FE-SEM and HR-STEM images support the Raman data so far confirming the presence SWCNTs.

3.3 Thermogravimetric analysis (TGA)

The purity and quantity of carbon nanotubes, respectively the metal catalyst content in the raw ablation material can be estimated by TGA [2].

The thermogravimetric analysis curves were recorded using a STA-8000 Perkin Elmer instrument. The thermogravimetric measurements of the ablation product were performed in the temperature range of 50-900°C with a 5°C/min temperature rate under synthetic air atmosphere (20% oxygen, 80% nitrogen) using 20 ml/min gas flow rate. The recorded curves are presented in the Figure 14, which shows the weight loss as a function of temperature (red line curve) and its derivative (blue line curve).

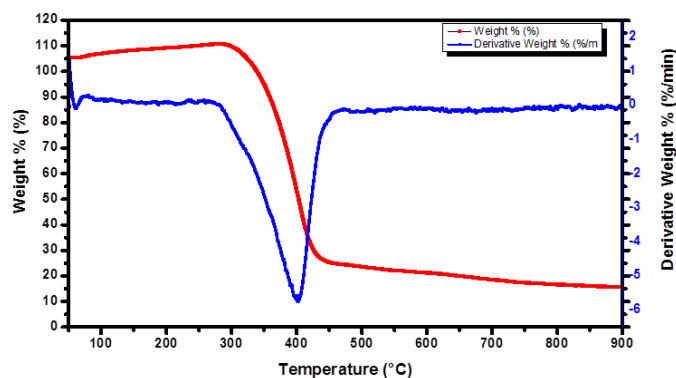


Fig. 14. TGA and DTG curves recorded in air for the raw ablation product SWCNTs.

We observed a weight loss of 84.6% corresponding mainly to SWCNTs burning. Most of the weight loss ~70 % occurred in the temperature range of 300-450°C where the SWCNTs and amorphous carbon burning take place [20]. The derivative blue curve confirmed this estimation and a low amount of amorphous carbon presence. The estimated yield of SWCNTs was ~60%. The residual weight percentage recorded at 900 °C was 15.40% corresponding to oxidized metal catalyst particles.

The TGA analysis confirmed the presence SWCNTs, amorphous carbon and metal catalysts particles supporting the Raman, FE-SEM and HR-STEM data.

4. Conclusion

In the present work we have shown the synthesis of good quality SWCNTs by KrF excimer laser ablation using Neon as ablation carrier gas.

The Raman measurements showed the presence of good quality SWCNTs, respectively the obtained SWCNTs are a mixture of metallic and semiconducting types, with the diameters within the range of 1.0 to 1.52 nm, and micrometers long.

FE-SEM and HR-STEM analysis showed the presence of individual and bundles of SWCNTs, amorphous carbon and metal catalyst nanoparticles in the ablation product. The diameters of the SWCNTs were within the range of 1.0 - 1.7 nm, while those of the bundles within the range of 2.5- 42 nm. The catalysts nanoparticles diameters contained in the ablation product were in the range of 1.6 to 19.75 nm.

The SWCNTs diameters obtained from Raman and HR-TEM analysis showed very close values.

The TGA analysis confirmed the presence of the SWCNTs, with an estimated yield of ~60%.

All the methods used for characterization support each other's results.

We proved for the first time that neon gas alongside other gases like argon, nitrogen, helium and krypton, is a suitable gas, but expensive one for good quality SWCNTs synthesis by excimer laser ablation.

Acknowledgments

This work was supported by Romanian Ministry of Education and Scientific Research, and by Executive Agency for Higher Education, Research, Development and Innovation Funding, under projects PCCA 2-nr. 166/2012 and ENIAC 04/2014. J. Al-zanganawee and T. Mubarak acknowledges the support from the ministry of the Higher Education and Scientific Research of Iraq, and the University of Dyjala.

References

- [1] S. Iijima, T. Ichihashi, *Nature* **363**, 603(1993).
- [2] D. Bethune, C.Kiang, M. Vries, G. Gorman, R. Savoy, J. Vazquez, R. Beyers, *Nature* **363**, 605-607 (1993).
- [3] Y. Tian, Optical properties of Single walled carbon nanotubes and Nanobuds, Theses, Aalto University (2012).
- [4] R. Saito, G. Dresselhaus, M. Dresselhaus, *Physical Properties of Carbon Nanotubes*, Imperial College Press (1998).
- [5] Y. Cheng, O. Zhou, C. R. Physique **4**, 1021 (2003).
- [6] H. Daia, and N. Franklin, *Applied Physics letters* **73**, 11 (1998).
- [7] S. Jain, S. Singh, D. Horn, V. Davis, M. Ram, S. Pillai, *Journal of Biosensors & Bioelectronics*, S:11 (2012).
- [8] H. Cheng, Q. Yang, *Carbon* **39**, 1447 (2001).
- [9] H. Derbal-Habak, C. Bergeret, J. Cousseau, J.M. Nunz, *Solar Energy Materials and Solar Cells* **95**, 1 (2011).
- [10] Z. Shi, Y. Lian, X. Zhou, Z. Gu, Y. Zhang, S. Iijima, L. Zhou, K. Yue, S. Zhang, *Carbon* **37**, 9 (1999).
- [11] R. Lacerda, A. Teh, M. Yang, K. Teo, N. Rupesinghe, S. Dalal, K. Koziol, D. Roy, G. Amaratunga, W. Milne, *Applied Physics Letters* **84**, 2 (2004).
- [12] W. Maser, E. Muñoz, A. Benito, M. Martínez, G. de la Fuente, Y. Maniette, E. Anglaret, J. Sauvajol, *Chemical Physics Letters* **292**, 4-6 (1998).
- [13] T. Oyama, T. Ishiim, K. Takeuchi, *Fullerene Science and Technology* **5**, 5 (1997).
- [14] D. Dorobantu, P-M Bota, I. Boerasu, D. Bojin, M. Enachescu, *Surface Engineering and Applied Electrochemistry* **50**, 5 (2014).
- [15] P-M. Bota, D. Dorobantu, I. Boerasu, D. Bojin, M. Enachescu, *Surface Engineering and Applied Electrochemistry*, **50**, 4 (2014)
- [16] D. Nishidea, H. Kataurab, S. Suzukia, K. Tsukagoshic, Y. Aoyagic, Y. Achibaa, *Chemical Physics Letters* **372**, 1-2 (2003).
- [17] A. Gorbunov, R. Friedlein, O. Jost, M. Golden, J. Fink, W. Pompe, *Applied Physics A* **69**,1 (1999).
- [18] P-M Bota, D. Dorobantu, I. Boerasu, D. Bojin, M. Enachescu, *Materials Research Innovations* **19**, 1 (2015).
- [19] J. Al-Zanganawee, C. Moise, A. Katona, D. Bojin, M. Enachescu, *Digest Journal of Nanomaterials and Biostructures* **10**, 4 (2015).
- [20] J. Al-Zanganawee, A. Katona, C. Moise, D. Bojin, M. Enachescu, *Journal of Nanomaterials* 2015, (2015).
- [21] M. Dresselhaus, G. Dresselhaus, R. Saito, A. Jorio, *Physics Reports* **409**, 47 (2005).
- [22] J. Maultzsch, H. Telg, S. Reich, C. Thomsen, *Physical Review B* **72**, (2005).
- [23] H. Kataura, Y. Kumazawa, Y. Maniwa, I. Umezu, S. Suzuki, Y. Ohtsuka, Y. Achiba, *Synthetic Metals* **103**, 2555-2558 (1999).
- [24] V. M. Irurzun, M. P. Ruiz, D. E. Resasco, *Carbon* **48**, 2873 (2010).
- [25] J. Lehman, M. Terrones, E. Mansfield, K. Hurst, V Meunier, *Carbon* **49**, 2581 – 2602 (2011).